



Supporting Online Material for
**The Great Divides: *Ardipithecus ramidus* Reveals the Postcrania of our
Last Common Ancestors with African Apes**

C. Owen Lovejoy,* Gen Suwa,* Scott W. Simpson, Jay H. Matternes, Tim D. White

*To whom correspondence should be addressed.

E-mail: olovejoy@aol.com (C.O.L.); suwa@um.u-tokyo.ac.jp (G.S.)

Published 2 October 2009, *Science* **326**, 73 (2009)

DOI: 10.1126/science.1175833

This PDF file includes:

SOM Text S1 to S3

Figs. S1 to S15

Tables S1 to S3

References

SOM Texts

TEXT S1. Bone Lengths and Indexes in *ARA-VP-6/500*

Nine long bones (other than phalanges) were recovered from the *ARA-VP-6/500* skeleton with sufficient preservation to allow accurate assessment of length based either on direct anatomical observation and measurement, or by standard quantitative techniques. These include a right radius (*ARA-VP-6/500-039* [its antimeric, *ARA-VP-6/500-018A* was recovered but less complete]), a right ulna (*ARA-VP-6/500-051*), a right femur *ARA-VP-6/500-005* and tibia *ARA-VP-6/500-003*, left metacarpals 1, (*ARA-VP-6/500-015*), 4 (*ARA-VP-6/500-010*), and 5 (*ARA-VP-6/500-036* [its antimeric, *ARA-VP-6/500-019* lacks only a base but length estimation is obviously unnecessary]), and left metatarsals 1 (*ARA-VP-6/500-089*) and 5 (*ARA-VP-6/500-067*). In addition, although no humerus was recovered for *ARA-VP-6/500*, we have estimated a length for this element because another nearly complete, slightly smaller specimen (*ARA-VP-7/2*) was also recovered. Descriptions of methods used in the assessment of each bone are as follows:

Right Radius (*ARA-VP-6/500-039*). Virtually complete, lacking only a portion of the radial head epiphysis. However, its styloid was crushed proximally and the bone suffered several fossilization cracks along its length. Original anatomical curvature was largely preserved except for mediolateral displacement by these cracks. Three authors (COL; GS; TW) independently estimated the bone's length by direct anatomical comparison to human and common chimpanzee radii. These estimates varied +/- 1 to 2 mm from each other within a range of 250-253 mm. We regard our estimate as highly accurate. Length: 250 mm.

Right Ulna (*ARA-VP-6/500-051*). Nearly complete but lacks a significant portion of its distal-most shaft and epiphysis. It also suffers from a number of displaced fossilization cracks that have produced a non-anatomical curvature. Because the distal ulnar shaft of hominoids lacks significant landmarks proximal to those associated with its distal epiphysis, we estimated bone length by regression from the specimen's radius, whose length we regard as highly accurate (see earlier) (ulna length = $.989$ [radius length] + 18.339 ; $r^2 = .990$; $N = 250$ for all anthropoids; ulna length = $.992$ [radius length] + 18.335 ; $r^2 = .991$; $N = 107$ for African apes and humans only). Both regressions yield identical estimates: 266 mm.

Right Tibia (*ARA-VP-6/500-003*). Complete including the intercondylar process but lacks a portion of its medial malleolus. The tibial plateau has been crushed posterodistally, and the shaft has suffered several fossilization cracks, but none has had a substantial effect on its length. Three authors (COL; GS; TW) independently estimated its length by direct anatomical comparison to human and common chimpanzee tibias. These estimates varied +/- 1-2 mm from each other in a total range of 262-264 mm. We regard our estimate as highly accurate. Length: 262 mm.

Right Femur (*ARA-VP-6/500-005*). Partially preserved but the shaft is complete from the base of its lesser trochanter to the tip of a substantial portion of its popliteal fossa which exhibits a visible and palpable lateral supracondylar line broken somewhat proximal to the gastrocnemius origin. Three authors (COL; GS; TW) independently estimated its length by direct anatomical comparison to human and common chimpanzee femurs. These estimates varied +/- 4-20 mm from each other (300-320). Although this range was reasonably small for an incomplete bone of

this length, we further investigated estimation of length based on the crural index (CI) of hominoids, which remains reasonably stable among these taxa because most elongation of the femur and tibia occurs at the knee epiphyses, which share the same *Hox* territories (1, 2, 34). The CIs of various primates are provided below. The mean CIs of the African apes and humans differ from each other only minimally in this sample (range of 81 to 84). Moreover, although the CI is higher in most other anthropoids, there is substantial evidence for negative allometry with increasing body mass in primates, with moderate coefficients of determination when examined both in all anthropoids and in Old World monkeys treated separately. Because the body mass of *ARA-VP-6/500* falls closest to that of chimpanzees, we have also estimated femoral length using the CI of chimpanzees. This yields an estimated length of 312 mm. There is substantial evidence, however, of moderate decrease in the length of the hindlimb in both African apes subsequent to the last common ancestor of *Gorilla* and humans (GLCA) and this may have had a slight effect on the CI of these taxa. Conversely, the human CI of 81 (which yields a femoral length estimate of 323 mm) is equally likely to have been affected by the dramatically elongated human hindlimb, and the human CI value may be inappropriate for that reason. However, because there is such minimal variation in the CI in African apes and humans, we regard the two extremes as a reasonable range of femoral length in *ARA-VP-6/500*, but we have used the more conservative estimate based on the chimpanzee CI in all calculations here and in the text. Estimated length: 312 mm.

The Crural Index in some Old World Primates

Taxon	N	Mean	S.D.
OWM	75	92	05
NWM	23	91	04
<i>Homo</i>	14	81	03
<i>Pan</i>	14	84	02
<i>Gorilla</i>	15	83	02
<i>Pongo</i>	18	88	03
<i>Hylobates</i>	11	87	02
<i>Proconsul</i>	1	92	

Humerus. No humerus was recovered from *ARA-VP-6/500*. However, a nearly complete humerus with intact proximal and distal ends and most of the shaft length preserved was recovered for the forelimb skeleton *ARA-VP-7/2*. That specimen, which was slightly smaller than *ARA-VP-6/500* (see below), is composed of three pieces, each of which fits to the others with only slightly eroded break surfaces with minimal separations. The minimum possible length of the specimen with these three pieces anatomically juxtaposed is 258. Morphological continuity associated with these joins suggests a likely additional spacing of a total of 6 mm between the three segments, with a maximum original length of 264 mm. The actual length of the specimen therefore varied between 258 (+ one mm for slight erosion if the joins are nearly perfect) and 264 if the joins are slightly off. We have estimated actual original length as the midpoint of these two

possible lengths: 261.5. As a means of potentially estimating the length of *ARA-VP-6/500* by multiple linear regression, we then estimated the length of *ARA-VP-7/2* using several metrics available from the radius, carpals and metacarpals of both specimens (including scaphoid, five metrics of the capitate, Mc4 length, and breadth of the distal radius). The resulting humeral length estimates for *ARA-VP-7/2* were either substantially over- or under-predictions of its length, and were heavily dependent on the composition of the sample used to compile the regression (see below).

Actual versus linear multiple regression values of humerus length using different extant taxa for compilation of the regression equation

	Predicted Length based on sample restricted to:					Actual Humerus length of sample
		<i>Pan</i>	<i>Homo & Pan</i>	Anthropoids	Hominoids*	
<i>ARA-VP-7/2</i>		251†	292	278	289	261.5
<i>ARA-VP-6/500</i>		251†	298	291	294	(278)
<i>Homo</i>	Mean	239	312	303	311	313
	N	30	30	30	30	30
	SD	8.6	13.6	24.3	22.5	21.5
<i>Pan</i>	Mean	306	308	328	324	306
	N	25	25	25	25	25
	SD	11.3	9.3	16.2	15.2	16.1
<i>Gorilla</i>	Mean	300	336	397	396	407
	N	24	24	24	24	29
	SD	16.6	23.2	44.6	37.7	41.8
<i>Pongo</i>	Mean	332	309	341	344	347
	N	17	17	17	17	19
	SD	15.9	21.4	43.2	37.3	26.7

*Gibbons excluded

†These values are identical only by virtue of rounding error

Inspection of the data generated for known humeral lengths in extant taxa reflected this same problem. An alternative method not dependent upon sample composition and relying on the very similar size of the two specimens is prediction of the length of *ARA-VP-6/500* by simple ratio. The following are simple proportions between bones preserved in both specimens [(*ARA-VP-6/500*) / (*ARA-VP-7/2*)]:

Bones compared:	Ratio:	Estimated Length:	Brachial Index:
Distal radius articular breadth (estimated in <i>6/500</i>):	1.075	281	89
Mc4 length (estimated in <i>6/500</i> : see below):	1.02	267	94
Geometric mean of six capitate dimensions:	1.075	281	89
Scaphoid length	1.08	282	89

A consideration that may bear on estimating humeral length is the brachial index (BI) in anthropoids (see below & Fig. S3). This index is strongly derived in both *Homo* and *Gorilla*, whereas its range in *Pan* spans the difference between the BIs of *Proconsul* (95) and *Equatorius* (86), strongly suggesting that its value in *Pan* is primitive for hominoids. There is no apparent relationship to body size in primates if the highly derived BIs of *Homo* and *Gorilla* are not considered (Fig. S3). The above four ratio values for estimated humeral length give corresponding BI values of 89 to 94. The BI of *A.L. 288-1* (based on reasonably accurate estimates of its radial length) is 92. The simple mean of all four of the above ratio estimates for *ARA-VP-6/500* is 277.8. We have therefore estimated length of *ARA-VP-6/500* humerus at 278, which gives a corresponding BI of 90. As there appears to be a general inclusive tendency of early hominids, early Miocene above branch quadrupeds, and *Pan*, to all have similar BIs, we regard our estimate of humeral length in *ARA-VP-6/500* using the above ratios to be reasonably accurate.

The Brachial Index in some Old World Primates

Taxon	N	Mean	S.D.
<i>ARA-VP-6/500</i>	1	90	
<i>A.L. 288-1</i>	1	92	
<i>Proconsul KNM-RU 2036</i>	1	95	
<i>Hylobates</i>	14	110	02
OWM	103	101	06
NWM	34	96	06
<i>Homo</i>	30	75	06
<i>Pan</i>	45	92	06
<i>Gorilla</i>	29	82	02
<i>Pongo</i>	19	102	04

Left Metacarpal 1 (*ARA-VP-6/500-015*). Preserved almost entirely intact, save for a small telescoping defect on its palmar surface. Although this defect had no effect on the dorsal dimensions of the bone, it appears to have slightly collapsed its length volarly, which may affect the metric we have used for Mc1 length. Although the original length may have been ~0.5 mm longer, we conservatively use the preserved length of 35.2 mm. Length: 35.2 mm.

Left Metacarpal 4 (*ARA-VP-6/500-010*). Complete save for a damaged proximal base. However, the fourth metacarpal of *ARA-VP-7/2* was intact and undamaged. Anatomical comparison of the two specimens by three authors (COL, GS, TW) gave agreement that the bone was originally 59.5-59.7 mm. Simple regression from the intact Mc5 of *ARA-VP-6/500* (see below) gives a prediction of 59.3 mm ($Mc4 = 1.062 Mc5 + .658$; $r^2 = .99$; $N = 258$). Length: 59.5 mm.

Left Metacarpal 5 (*ARA-VP-6/500-036*). Intact and perfectly preserved. Length: 55.3 mm.

Left Metatarsal 1 (*ARA-VP-6/500-089*). This is a damaged but nevertheless complete first metatarsal. The head is entirely intact, and although the basal articular surface is damaged, the

major portion of its dorsal joint surface is well preserved. However, the most plantar part of the joint surface, in particular the plantar angle that bears the typical rough oval prominence for the insertion of the fibularis longus tendon, and a small portion of its superolateral surface have been crushed medially, artificially increasing the curvature of its proximal joint surface. This has slightly increased the bone's length if measured from its most inferior proximal point to the distal head. However, the actual maximum length is preserved at its more intact superior portion to the distal end. Length: 55.6 mm.

Left Metatarsal 5 (ARA-VP-6/500-067). Although damaged, this Mt5 shaft is sufficiently preserved to permit reliable estimation by regression; *i.e.*, it is complete from the anterior edge of its Mt4 facet to the base of its medial cornua, two landmarks that provide a reliable relationship with overall bone length in hominoids ($r = .78$; $N = 30$ chimpanzees, 30 gorillas, 30 humans). Length: 63.7 mm.

Text S2. Potential Hox Pathways Involved in Ray Evolution in Hominoids

Independent elongation of the first ray to enhance manual opposition is likely to be a complicated developmental pathway. Up-regulation of only *Hoxd13* or one or more of its targets simultaneously shortens the posterior metacarpus, thereby negatively impacting its role in suspensory locomotion. Indeed, compared to body size, the Mc1s of all extant large bodied hominoids are of approximately similar length (Fig. S10), except for those of the orangutan, which are considerably longer. While this is explicable by simple upregulation of *Hoxd11* or one or more of its targets, extant apes also show soft tissue involution of the first ray--with frequent failure to fully manifest tendons of the *m. flexor pollicis longus*. This is also true of the orangutan. Loss of the anlage of such a tendon (by downregulation of *Hoxa13* or *Hoxd13*) might account for the redirection of the original muscle mass to the common deep flexors of the posterior digits. It cannot, however, account for elongation of the Mc1 in the orangutan. Figs. S4 and S5, however, provide a possible solution--it can be seen that the other long bones of the orangutan forelimb are also much elongated as they are in the gibbon. Elongation of the orangutan Mc1 is therefore likely to be a systemic adaptation involving greater expression of GH or IGF1 receptors in the growth plates of all the bones of the forelimb, including those of all five metacarpals. The favorably proportioned human first ray is likely to have been achieved largely by marked reduction of the posterior rays via down-regulation of *Hoxd11* or its targets, and the markedly shortened human antebrachium is likely a Type 2 manifestation of this phenomenon (1). The greater relative length of the Mc1s (and Mt1s) of Old World monkeys and *Proconsul* therefore suggest that the autopod must be, to some degree, more developmentally isolated from the global effects of systemic anabolic changes than are more proximal limb elements, thereby facilitating local modification by targeted gene expression (2). This would seem to contribute to the remarkable plasticity in autopod structure achieved by many mammals (compare the highly derived autopods of chiroptera and primate primates to their more conservative proximal limb elements).

Text S3. Invagination versus Length Reduction in the Lumbar Spines of Hominoids

Dorsalization of the lumbar transverse process in Miocene hominoids can now be seen to have been a complex pleiotropic effect of anterior invagination of the thoracic column for more posteromedial scapular positioning in order to facilitate bridging and clambering and not suspensory locomotion or vertical climbing. Anterior subduction of costovertebral junctions into the thorax simultaneously alters external thoracic form and facilitates translation of the scapula posterodorsally (for improved scapulohumeral circumduction). Along with craniocaudal shortening of each centrum, this stiffens the entire vertebral column, compensating for reduction of erector spinae mass, which must have remained substantial prior to the last common ancestor of *Gorilla* and humans (GLCA) despite tail loss (3, 4). In addition, the associated broadening of the thorax to accommodate posteromedial translation of the scapula provides a compensatory increase in the moment arms of the abdominal obliques, serratus posterior, and iliocostalis muscles that control lateral flexion of the free vertebrae during bridging, which can now be viewed as the primary truncal adaptation in the GLCA. More dramatic rigidity of the lumbar column via lumbar number reduction, individual element immobilization, and conversion of the iliac crest/thorax gap to the equivalent of a single intercostal space, is seen only in extant African apes and *Pongo*, and appears to have emerged secondarily to stabilize the abdomen and thorax during suspensory locomotion and vertical climbing (5). This explains the retention of a relatively long lumbar column in *Nacholapithecus* (6, 7), as well as full ventral invagination of the column in *Dryopithecus*, despite the latter taxon's simultaneous retention of metacarpophalangeal dorsiflexion and associated palmigrady (8).

In retrospect, we can now ask how such reorganization, which greatly compromises erector spinae function, could have ever, of itself, been perceived as a product of positive selection for suspensory locomotion, save explanations founded in adaptationism. It was instead clearly a manifestation of the primary embryogenetic shifts in bauplan recruited to enhance shoulder mobility. The inevitable spinal invagination that accompanied such posterior translation, however, also "passively" rigidified the thorax, thus at least partially compensating for simultaneous erector spinae reduction (5, 9). This may also account for why the lumbar transverse processes of *Hylobates*, the most preeminent of all suspensory arborealists, remain restricted to the pediculocentral junction, while those of large-bodied hominoids have become entirely pedicular. These shifts appear now to have occurred in parallel within demonstrably different locomotor contexts.

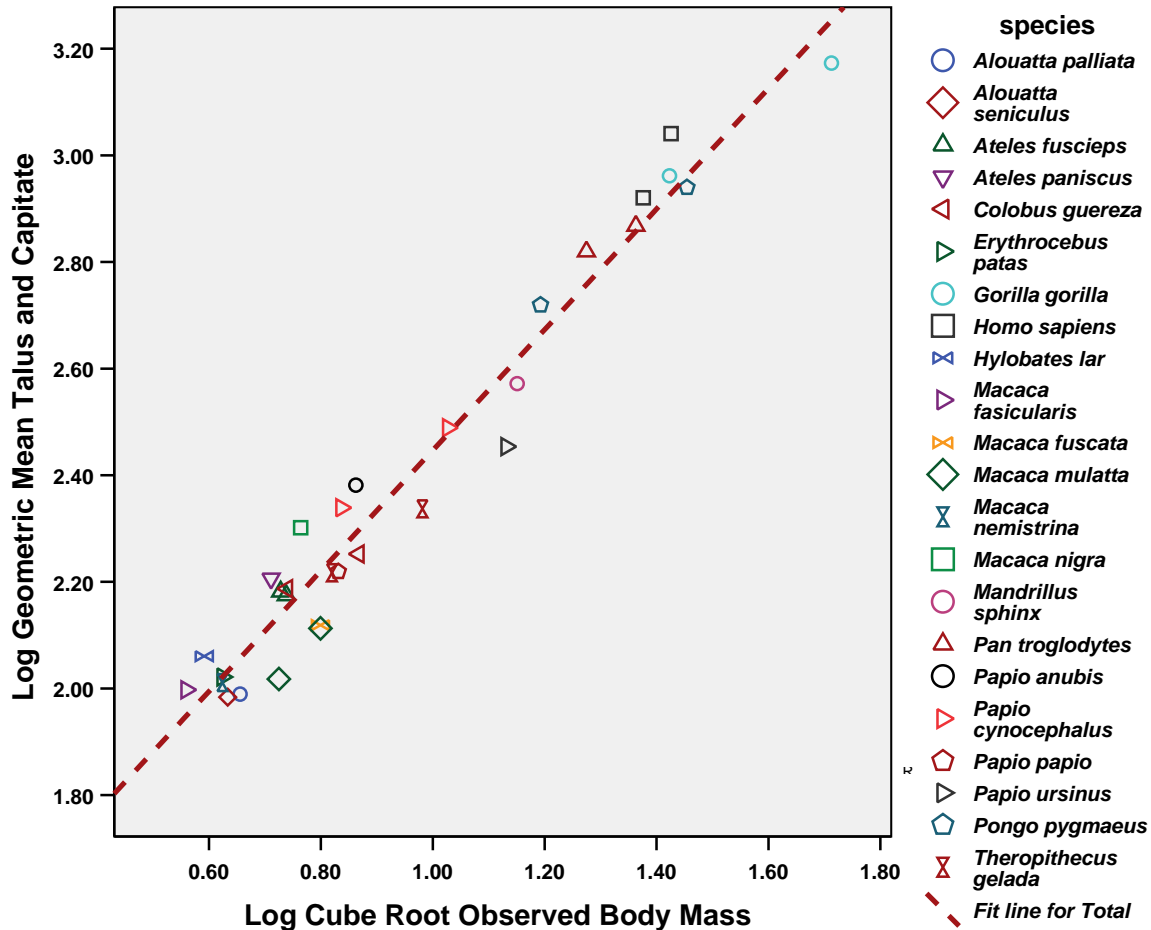


Figure S1. Relationship between Linear Metrics and Body Mass in Anthropoids. Natural log-log scatterplot of the cube root of body mass and the geometric mean (GMCT) of two separate metrics, one for the capitate (the geometric mean of five metrics: proximodistal length; height and breadth of Mc3 articular surface; height and breadth of the capitate head), and four of the talus (the geometric mean of the length and breadth of the trochlea and the length and breadth of the posterior calcaneal facet) (see below for further details of these metrics). Plotted are the single-sex means for each listed species (body mass data from (10)). For all anthropoids only, the regression equation ($.827 \log \text{GMCT} - 1.022$) gives body mass estimates of 50.5 Kg (50% confidence interval: 44.6–58.3 Kg) for ARA-VP-6/500 and 26.9 for A.L. 288-1. Estimates based on regression equations using only large-bodied hominoids (gibbons excluded) give similar results to the latter estimates for ARA-VP-6/500: 52.1 Kg for all hominoids, and 51.0 Kg for females only. The latter estimate is used for the calculations shown in Table S3. Using only hominoids to predict the body mass of A.L. 288-1, however, yields probable underestimates (22.9 Kg for all hominoids; 24.3 Kg for females only) because this specimen falls well below the actual body mass range of our hominoid sample (smallest value = female *Pongo pygmaeus* at 35.8 Kg). For this reason we have used the 26.4 Kg estimate derived from all anthropoids for A.L. 288-1 in Table S3, which is closer to other published estimates (11). Throughout the notes and figures that follow, estimates of body size (e.g., mass) are based on these calculations from the capitate and talus of the various taxa used in the analyses. The actual metrics of the capitate

and talus were taken as follows. For *ARA-VP-6/500*, casts of the capitate and talus were used so that metrics on these and the comparative materials could be cross-checked for comparability. The dimensions for the *ARA-VP-6/500* capitate were as follows: Mediolateral breadth of the head taken parallel to a tangent to the bone's dorsum (11.3); Dorsopalmar height taken perpendicular to previous metric (9.8); Dorsopalmar height of the Mc3 articular surface (subchondral bone only)(16.2); Mediolateral breadth of the Mc3 articular surface (subchondral bone only but inclusive of any adjacent facet surface for trapezoid) taken at the dorsopalmar midpoint of the bone's articular surface (9.4); Maximum anteroposterior length of the bone (19.6). Dimensions for the *ARA-VP-6/500* talus were as follows: Proximodistal length of the trochlea taken along its AP midaxis (subchondral bone only) (25.9); Mediolateral breadth of the trochlea at midpoint of previous metric (subchondral bone only) (21.5); Maximum subchondral bone length of calcaneal facet (mediolateral) (25.1); Breadth of calcaneal facet taken perpendicular to, and at the midpoint of, previous metric (16.9).

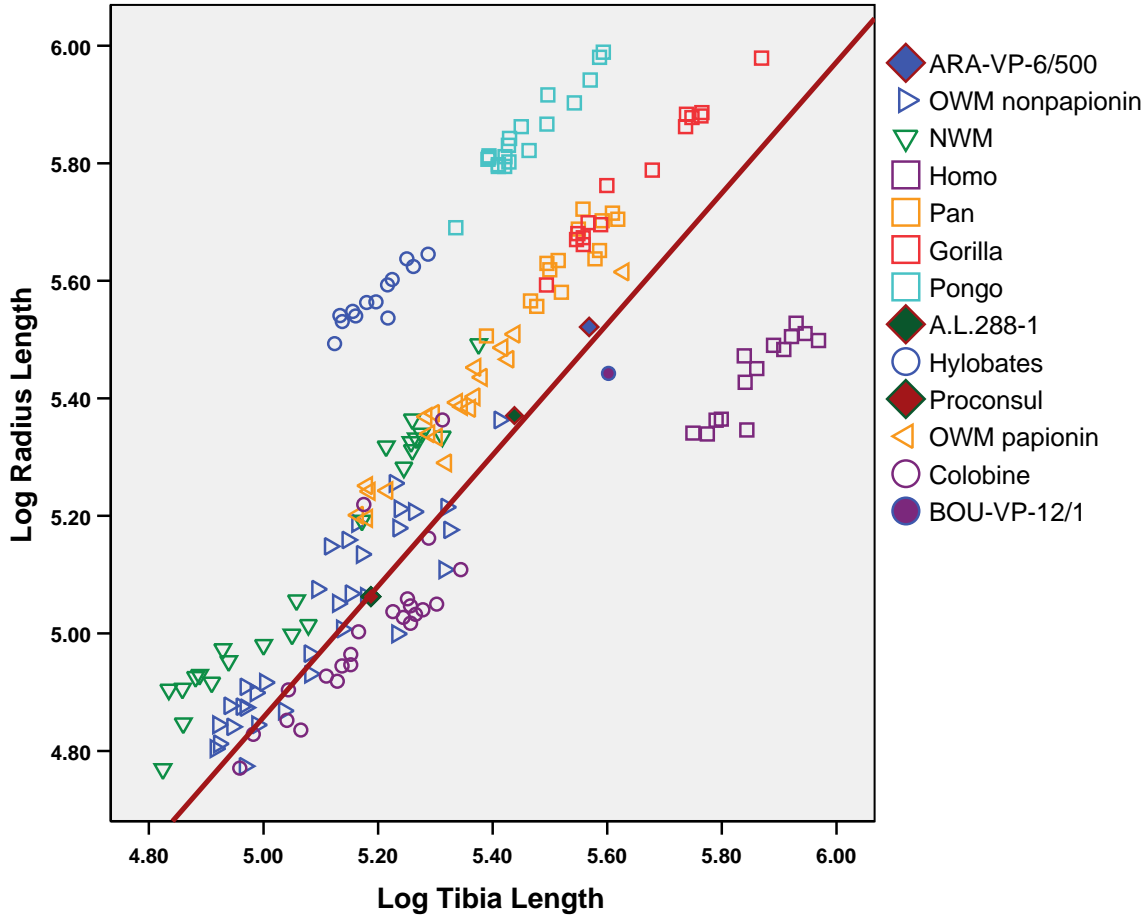


Figure S2. Limb Proportions in Anthropoids. Natural log-log scatterplot of radius length and tibia length in anthropoids. A regression is plotted for non-papionin Old World monkeys (RMA: $y = 1.11x - .71$; $N = 55$; $r = .829$), suggesting that limb proportions of *Proconsul*, *ARA-VP-6/500*, and the last common ancestor of *Gorilla* and humans (GLCA) remained primitive as in above branch quadrupeds. Note that *A.L. 288-1* retains these same proportions. Both extant African apes show radial elongation and/or tibial reduction. Their greater disproportion in orangutans and gibbons are obvious. Humans show dramatic abbreviation of the antebrachium, and data also confirm that *BOU-VP-12/1* exhibits human-like hindlimb elongation, but still lacks human-like antebrachial abbreviation (12). Ape intermembral indices (IMI) suggest global forelimb elongation *and* hindlimb abbreviation since the GLCA (*cf.*, Table S3), and can be confirmed by comparison of each bone to estimated body mass (see Figs S4–S6). Note that the colobine data [purple open circles] suggest hindlimb elongation in Asian species for leaping (*e.g.*, *Trachypithecus*, *Presbytis*). Note also that papionins (orange horizontal triangles) show relative elongation of the radius, but for obviously different reasons than African apes. Force plate data for vervets (*Cercopithecus aethiops*, a terrestrial nonpapionin) are unusual among anthropoids in the degree to which their trailing forelimbs show net propulsion during gallop (13). Based on this observation, a reasonable presumption is that papionin forelimb elongation provides additional power during rapid terrestrial locomotion, although papionins themselves have not been tested. The large papionin outlier is a male mandrill.

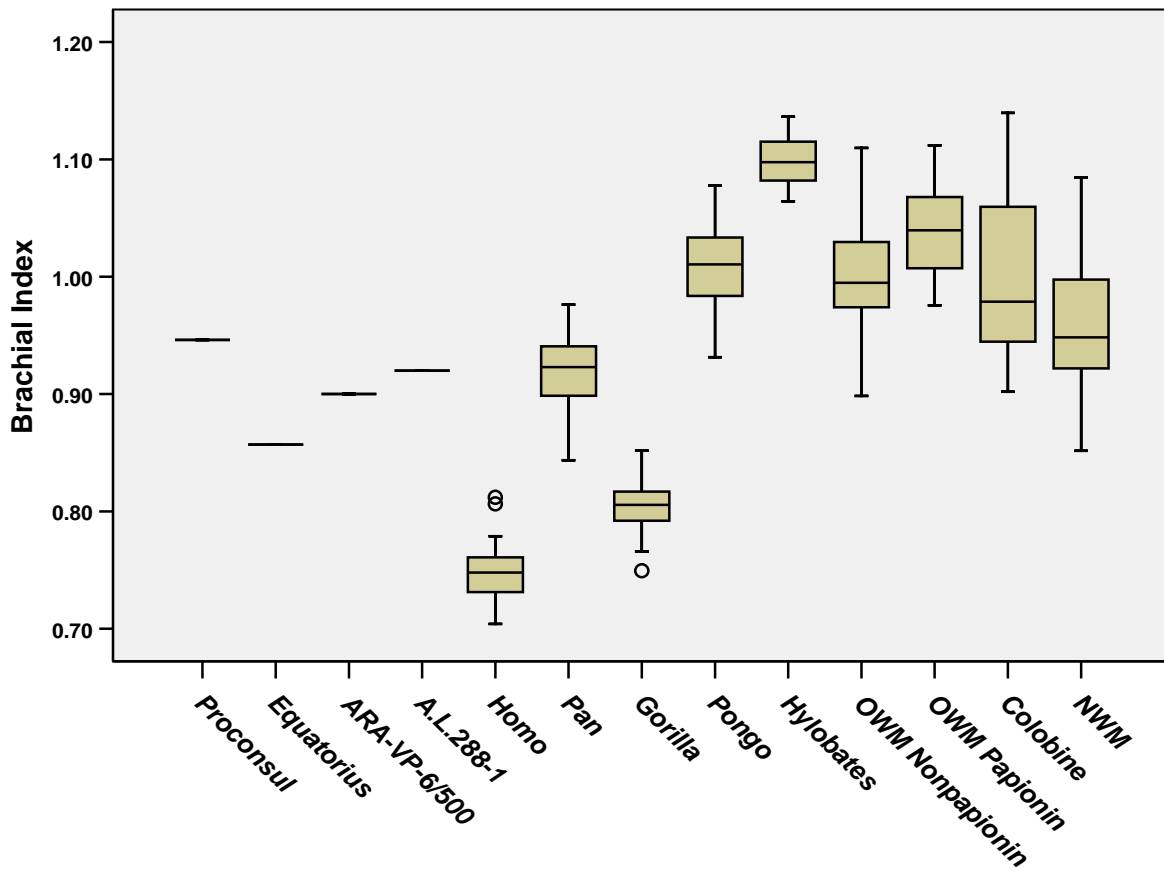


Figure S3. The brachial index in anthropoids. Brachial index (BI) = radius length/humerus length. The markedly abbreviated radius of *Homo* is obvious. However, relative radial length in *Gorilla* is also striking. Inspection of humeral and radial lengths relative to body size (Figs. S4, S5) suggests that the gorilla humerus has become elongated and its radius perhaps slightly abbreviated, even though the general length of its entire forelimb has been increased for suspensory locomotion. These changes relocate the elbow more distally within an arm of equivalent length, allowing greater loads to be carried by the humeral diaphysis rather than by the elbow joint. In contrast to *Gorilla*, Asian apes (*Pongo* and *Hylobates*), have very high brachial indexes, suggesting a unique locomotor history unlike that of the African apes, which based on data presented elsewhere, appear to have experienced an extensive period of bridging and above branch locomotion prior to their adoption of suspensory locomotion. Radius reduction in *Homo* is likely a Type 2 consequence of length reduction of the posterior metacarpals (for increased manual dexterity and pollical opposition), whose growth plates share *Hoxd11* expression with the distal radius and ulna (cf., Fig. S4) (1). In this figure and in Fig. S11, boxes represent 25th and 75th percentiles, whiskers are 5th and 95th percentiles, and the transverse line is the median. Cases with values between 1.5 and 3 box lengths from the upper or lower edge of the box are shown as open circles. Cases with values more than 3 box lengths from the upper or lower edge of the box are shown as asterisks. The box length is the interquartile range.

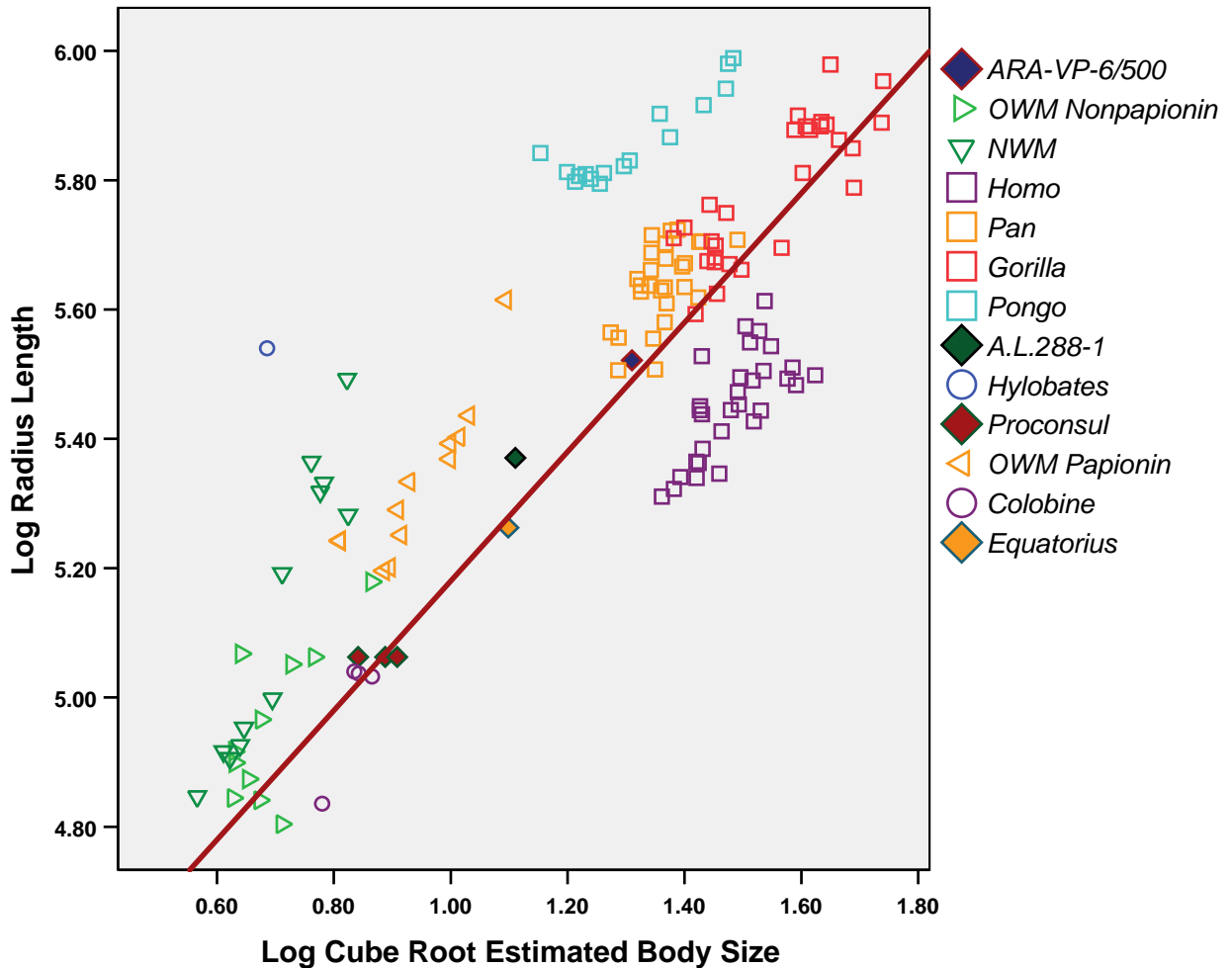


Figure S4. Radius Length Relative to Body Size in Anthropoids. Natural log-log scatterplot of radius length and the cube root of estimated body size. The body mass of *Proconsul* specimen *KNM-RU 2036* was judiciously estimated by Ruff and colleagues (14, 15) who give three potential values. The *Equatorius* data are from Ward *et al.* (16). All three have been plotted here along with those for other taxa derived by methods described in the legend of Fig. S2. A reference line with a slope equal to one has been fitted through *Proconsul*. Note that this line also passes through the *ARA-VP-6/500* point, confirming an absence of radial elongation in early hominids, and by extension, the last common ancestor of *Gorilla* and humans (GLCA) as well. *Pan* and *Gorilla* both exhibit an elongated radius. However, their brachial indices differ substantially (cf., Fig. S3), suggesting evolution of this adaptation in parallel after separation from the GLCA.

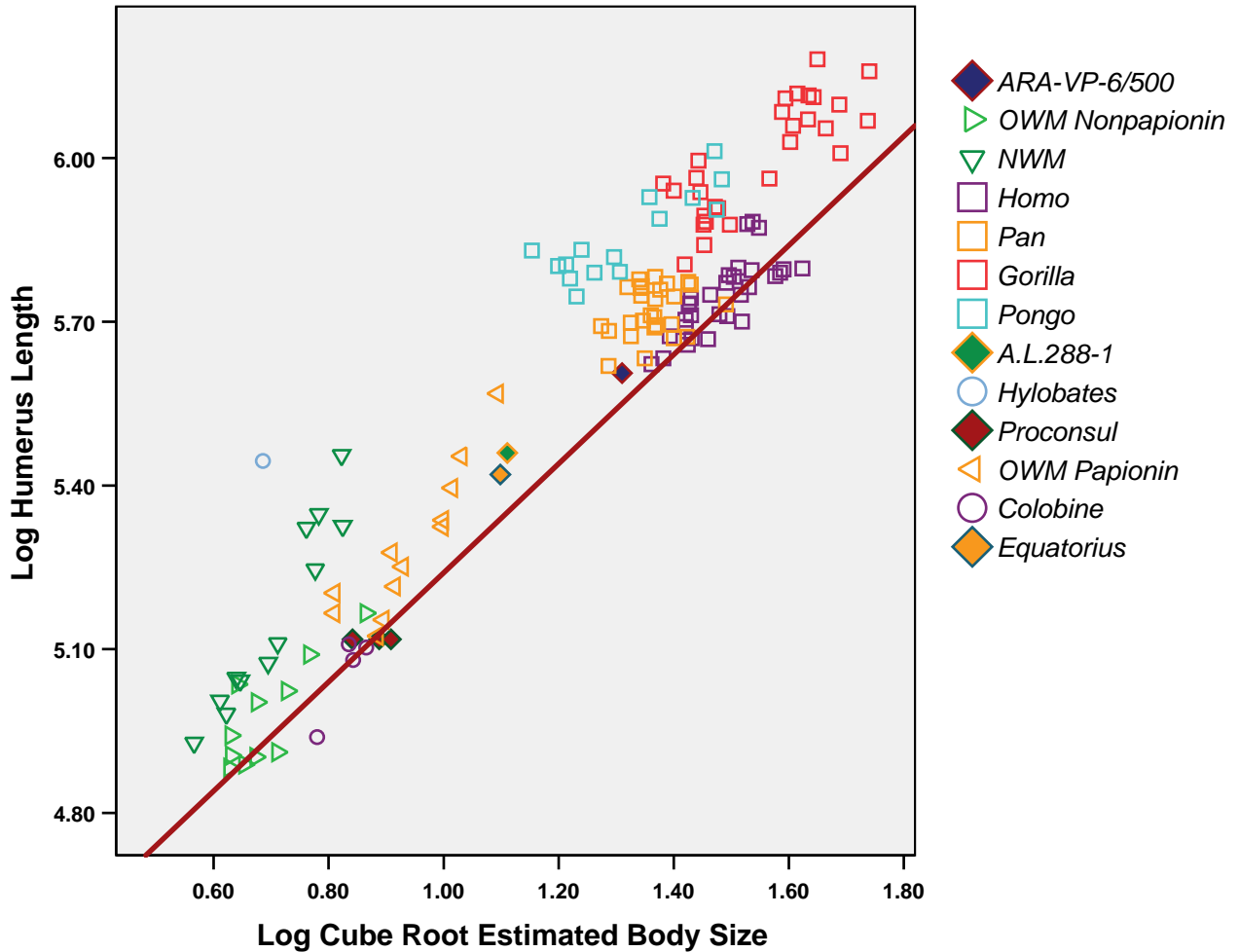


Figure S5. Humerus Length Relative to Body Size in Anthropoids. Natural log-log scatterplot of humerus length and the cube root of estimated body size. A reference line with a slope equal to one has been fitted through *Proconsul* (see the legend of Fig. S4 for body size estimates in *Proconsul*). Humerus length is clearly elongated in *Pongo* and *Gorilla*, whereas it appears to have remained unchanged relative to body size in *ARA-VP-6/500* and *Homo*. It has been elongated to a lesser extent in *Pan* and Old World monkey papionins. Several colobines are hidden by the three *Proconsul* points. The position of *A.L. 288-1* may simply be either individual deviation or an allometric effect of the specimen's unusually small body size, as it is unlikely that humeral length would have become elongated after *ARA-VP-6/500* and then secondarily shortened again in *Homo*. This may have misled a number of observers with respect to interpretations of early hominid locomotion and phylogeny [see, for example (17)]. The same may be true for *Equatorius*.

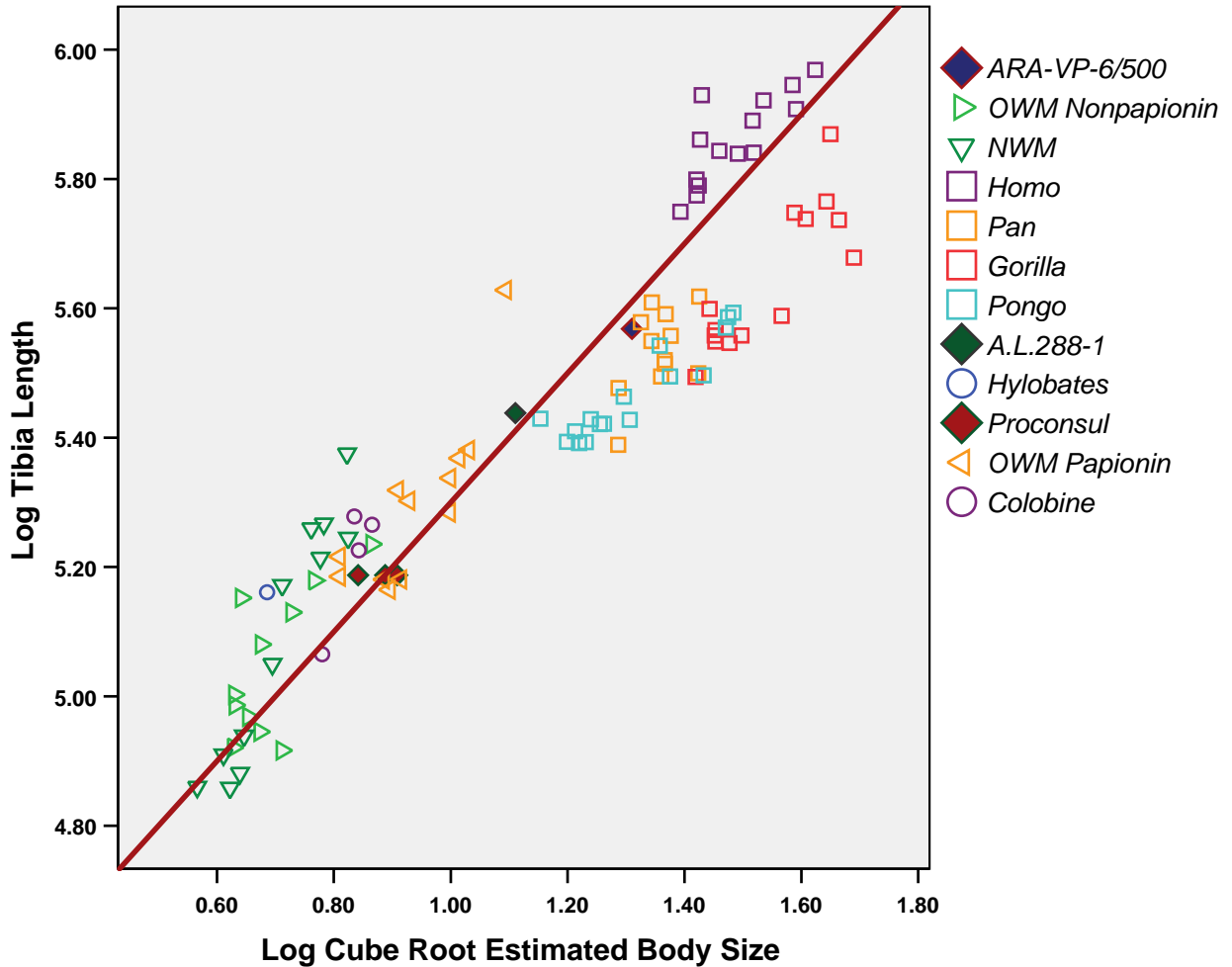


Figure S6. Tibia Length Relative to Body Size in Anthropoids. Natural log-log scatterplot of tibia length and the cube root of estimated body size. A reference line of slope equal to one has been fitted through *Proconsul* (see the legend of Fig. S4 for body size estimates in *Proconsul*). Tibia length is clearly abbreviated in *Pongo*, *Pan*, and *Gorilla*, and perhaps slightly in *ARA-VP-6/500*. However, when combined with the position of *A.L. 288-1*, it probably represents only individual deviation with the hindlimb having remained unchanged in hominids from its relative length in the last common ancestor of *Gorilla* and humans (GLCA).

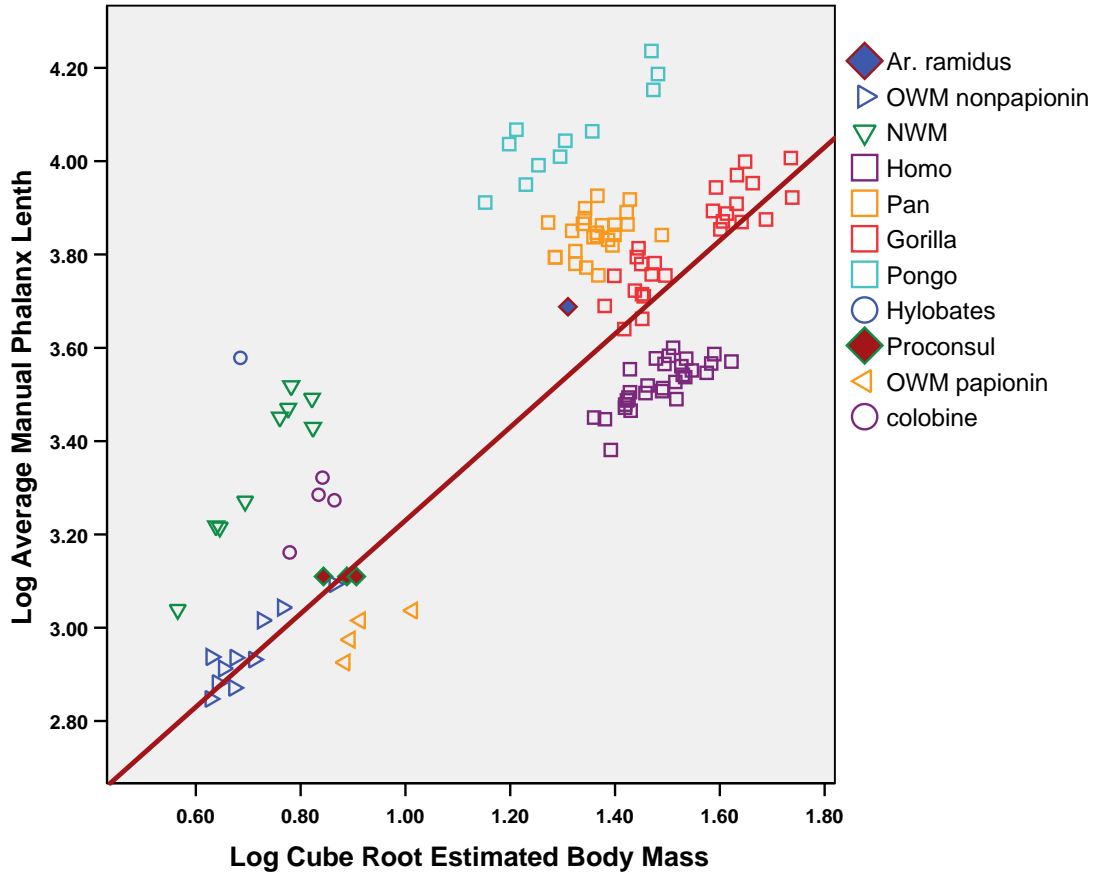


Figure S7. Manual Phalanx Length Relative to Body Size in Anthropoids. Natural log-log scatterplot of the cube root of estimated body mass and average length of six proximal and intermediate manual phalanges recovered for both *ARA-VP-6/500* and *KNM-RU 2036* (see the legend of Fig. S4 for body size estimates for this specimen). Phalanges are the proximals from rays 2, 3, and 4 and the intermediates from rays 3, 4, and 5. A line of slope equal to one has been fitted through *Proconsul*. It demonstrates elongation of the manual phalanges in *Gorilla*, *ARA-VP-6/500* (and thereby presumably the last common ancestor of *Gorilla* and humans (GLCA)), and colobines, with further elongation in *Pan* but substantial abbreviation in *Homo*. The phalanges of *Pongo* are strikingly elongate. Those of a small sample of terrestrial papionins are also abbreviated.

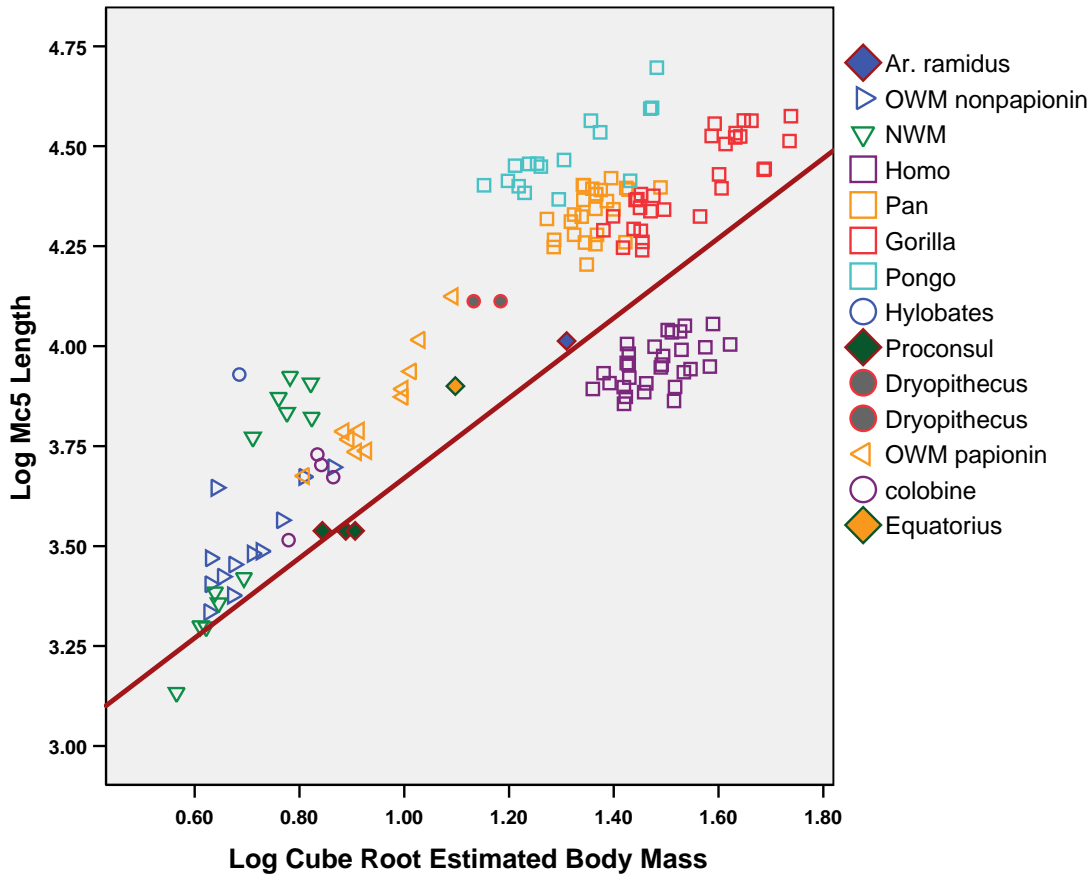


Figure S8. Posterior Metacarpal Length Relative to Body Size in Anthropoids. Natural log-log scatterplot of the cube root of estimated body mass and Mc5 length (representing the posterior metacarpus) in anthropoids. A line of slope equal to one has been fitted through *Proconsul* (see the legend of Fig. S4 for body size estimates in *KNM-RU 2036*; an Mc5 for this specimen was not preserved--the value used here is regressed from its Mc4 (data not shown)). Although both Old World monkeys (OWMs) and apes fall above this line, *Pan* and *Gorilla* metacarpal lengths are unlikely to have scaled as enlarged OWMs because the latter are above branch quadrupedal, palmigrade, metapodial fulcrumators. Moreover, note that *Proconsul* falls below nonpapionin OWMs of equivalent body size. This suggests relatively shorter metacarpal lengths for enhanced grasping, and at least some reduction in reliance on metapodial fulcrumation. Relatively short posterior Mcs contribute to better opposition with the pollex. These are likely transitional adaptations to clambering and branching in *Proconsul*, consistent with tail loss in this genus (18). *ARA-VP-6/500* appears to have retained the primitive condition as exhibited in *Proconsul* and presumably the last common ancestor of *Gorilla* and humans (GLCA). Both *Pan* and *Gorilla* show post-GLCA differential elongation of their posterior metacarpus, almost certainly in response to secondary development of SL. This hypothesis is robustly supported by data for the metatarsus (see Figs. S13, S14), which do not show equivalent elongation and thus imply increased reliance on pedal grasping, an obvious adaptation to both suspensory locomotion and vertical climbing. The position of *Equatorius* (16) suggests that it also may have had slightly longer relative posterior metacarpal lengths, either for metacarpal

fulcrumation or as part of a general forelimb elongation as in *Nacholapithecus* (6). Its position on the graph suggests a possible adaptation of the posterior metacarpus as seen in *Colobus*. Two points have been plotted for *Dryopithecus*, representing the upper and lower limits of body size estimates for the specimen shown here (19). The even more extreme metacarpal length in this genus is best interpreted as probable secondary elongation, because *Dryopithecus*, unlike *Nacholapithecus*, exhibits both ulnar withdrawal and lumbar transverse process relocation consistent with substantial changes in locomotor pattern. Its metacarpal elongation therefore more likely reflects a general Miocene trend toward increased reliance on suspension and an arboreal propulsive forelimb, rather than the more conservative pattern exhibited by hominoids prior to the GLCA. The morphology of *Dryopithecus* is therefore likely a parallelism with post-GLCA African apes. Note that New World monkeys show two distinct distributions: the longer of the two are *Ateles*, whereas the shorter are largely *Alouatta*, which may be a reasonable proxy for some aspects of *Proconsul* locomotion. It is worthy of note that locomotor divergence in atelines appears to parallel that in African apes and hominids, with one clade retaining more primitive proportions (*i.e.*, *Alouatta*) while others develop more substantive adaptations to suspension (*Ateles* and *Brachyteles*).

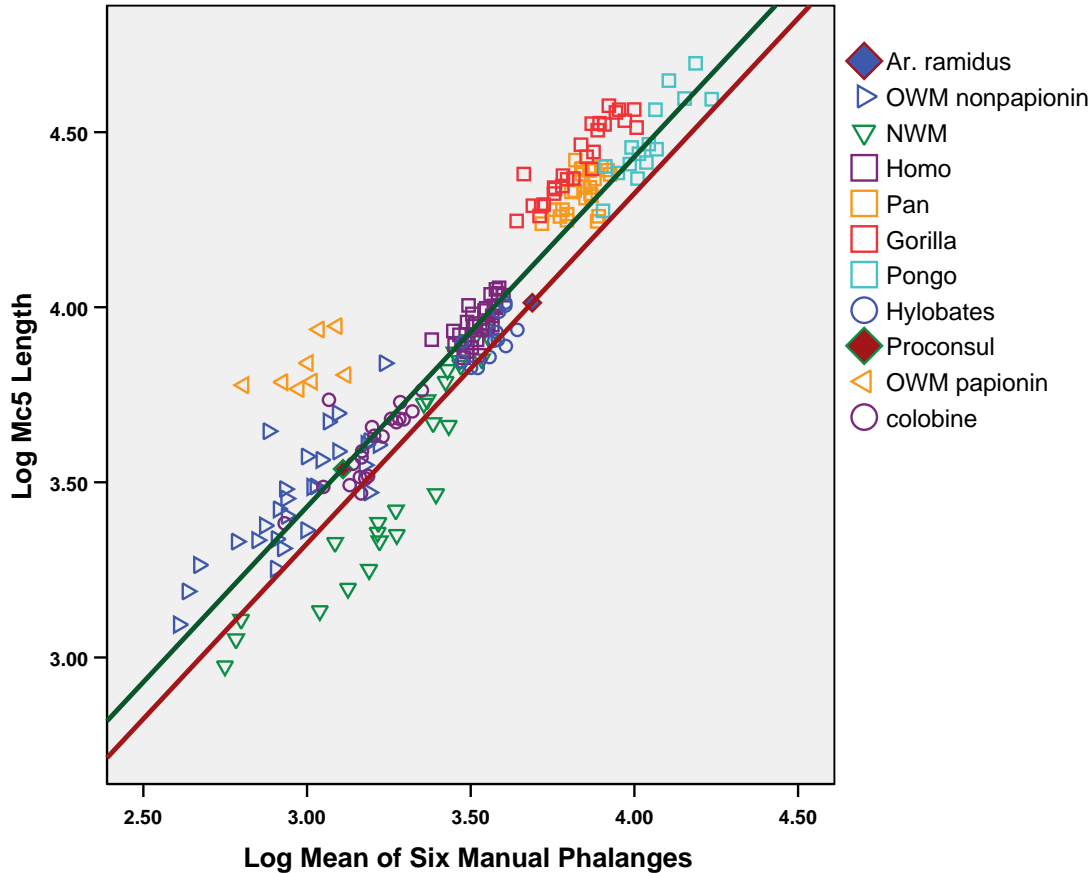


Figure S9. Phalangeal-Metacarpal Proportions in the Anthropoid Hand. Natural log-log scatterplot of Mc5 length and the average length of six manual proximal and intermediate phalanges. Lines of slope equal to one have been fitted through *Proconsul* and *Ar. ramidus*. Compared to *Proconsul*, phalangeal length has increased in *Ar. ramidus* and presumably therefore the last common ancestor of *Gorilla* and humans (GLCA). Both phalangeal length and metacarpal length have been reduced in *Homo*, whereas the posterior metacarpus has been demonstrably elongated in both African apes. The position of *Gorilla* may also represent some reduction in phalangeal length since the GLCA. Both the posterior metacarpals and the phalanges of *Pongo* are elongated. Considering its nearly comparable body size, the elevation of *Pan* above *Ar. ramidus* is striking, attesting to its advanced post-GLCA adaptation to suspensory locomotion and vertical climbing primarily by substantial elongation of its posterior metacarpus. Note the very distinctive metacarpal/phalangeal ratios of papionins (orange triangles), likely reflecting the coupling of metapodial elongation for increased power during forelimb propulsion with phalangeal reduction, both of which tend to be characteristic of some terrestrial species.

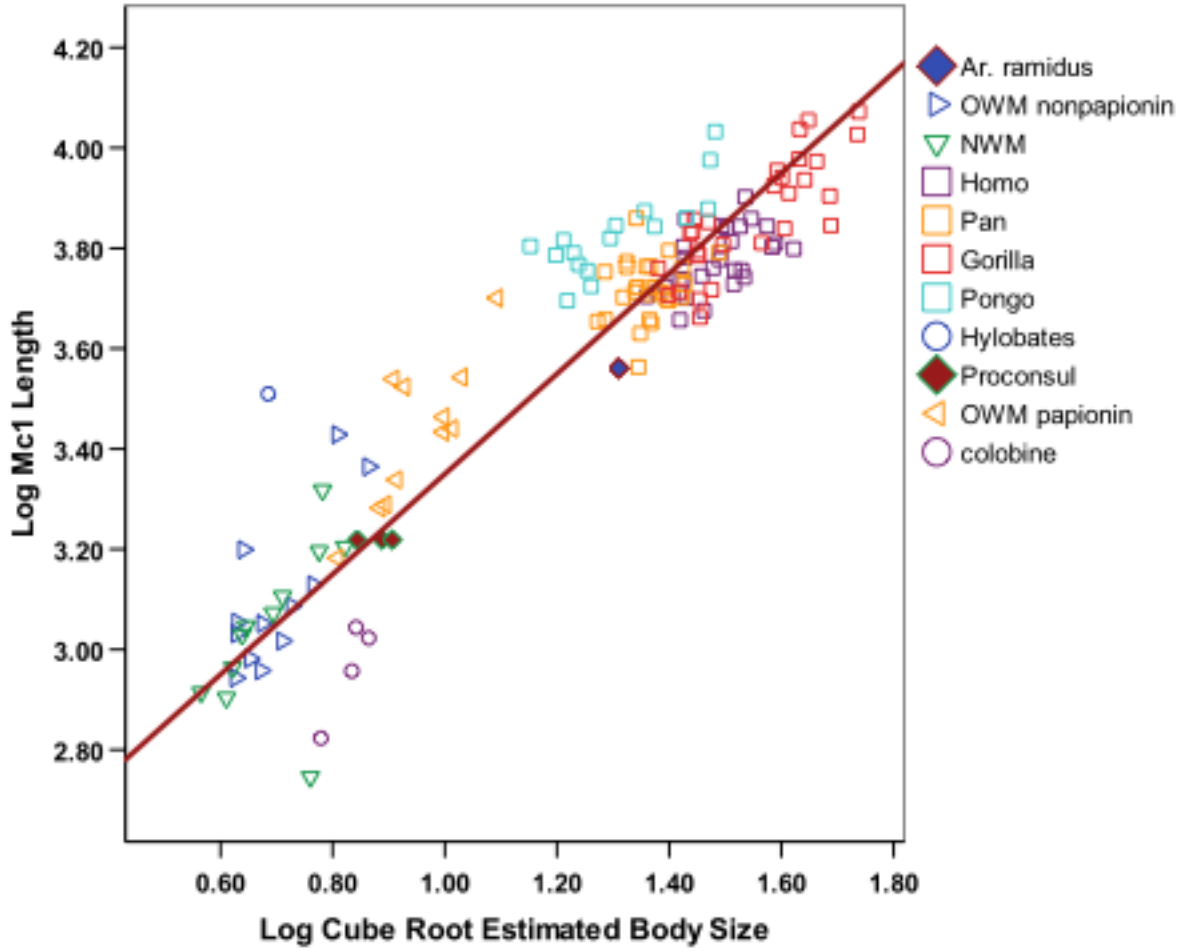


Figure S10. Mc1 Length Relative to Body Size in Anthropoids. Natural log-log scatterplot of the cube root of estimated body mass and Mc1 length. A line of slope equal to one has been fitted through *Proconsul*. See the legend of Fig. S4 for body size estimates in *KNM-RU 2036*. For discussion see text.

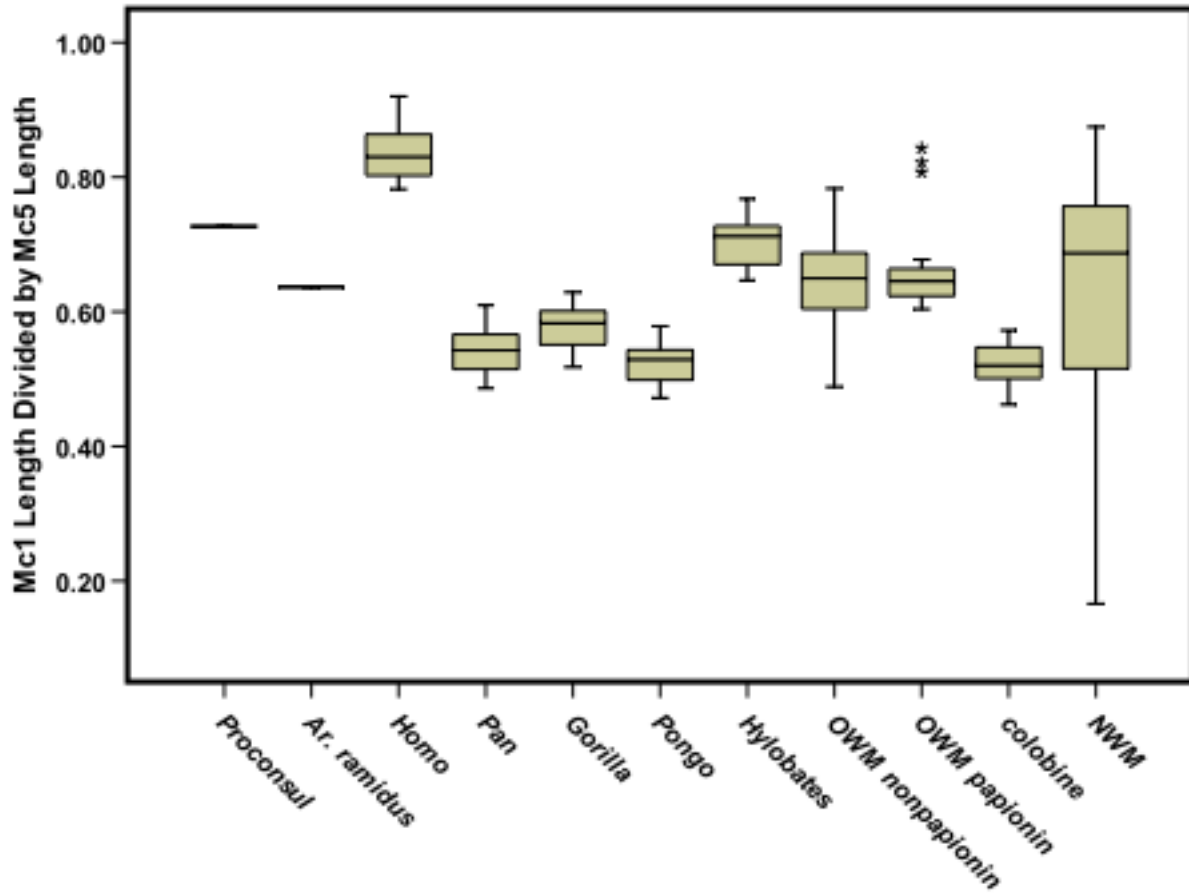


Figure S11. Relative Mc1 and Posterior Digit Proportions in Hominoids. Box and whisker plots of the ratio of Mc1 to Mc5 length. African apes show a relatively shorter first ray compared to their elongated posterior metacarpals. For definition of box plot symbols see Fig. S3.

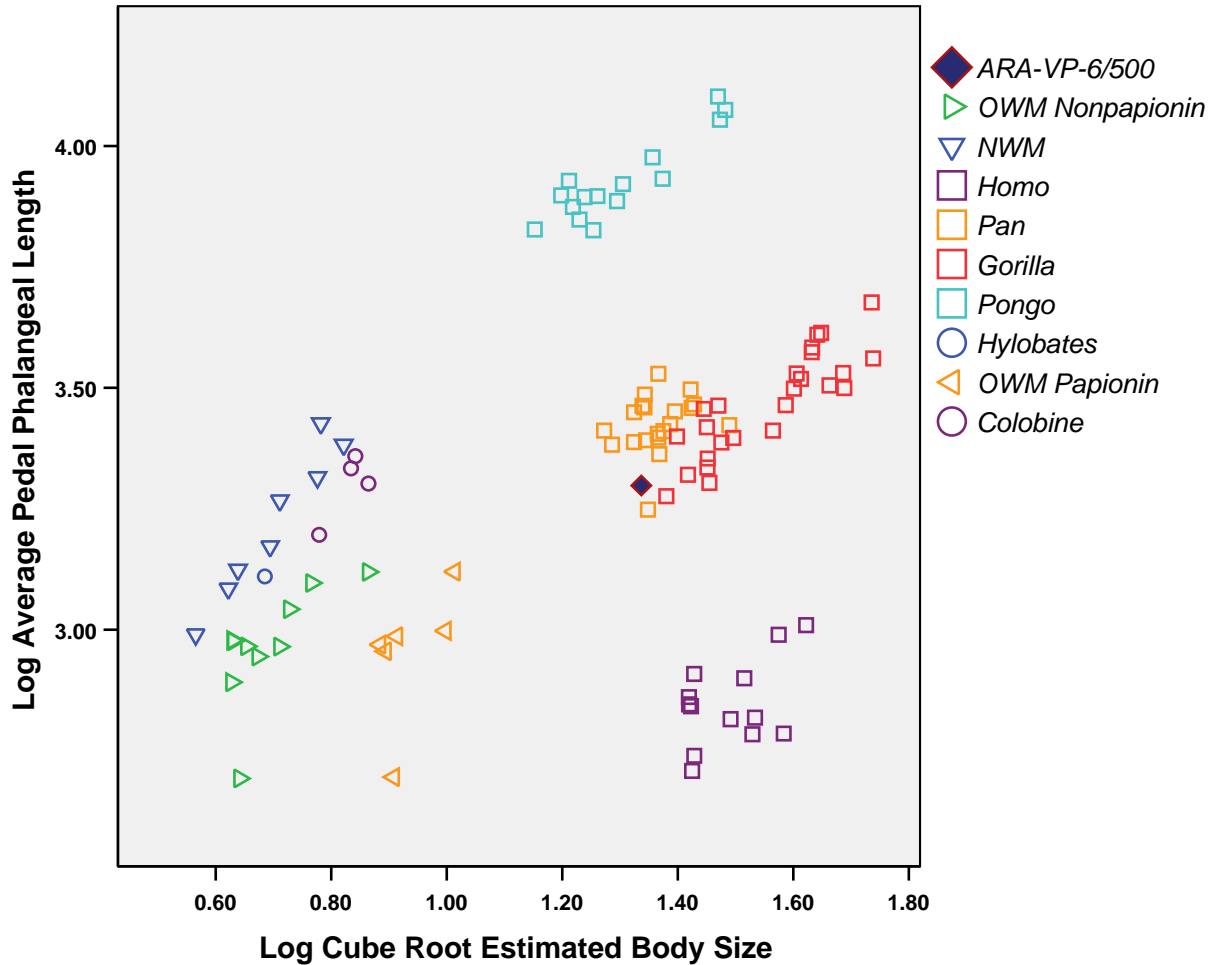


Figure S12. Pedal Phalanx Length Relative to Body Size in Anthropoids. Natural log-log scatterplot of the cube root of estimated body mass and average length of six proximal and intermediate pedal phalanges recovered for *ARA-VP-6/500* (data unavailable for *KNM-RU 2036*). Phalanges are the proximals and intermediates from rays 3, 4, and 5. Comparison of these data to those shown in Fig. S7 suggests a general equivalence in size of manual and pedal phalanges in most species with the exception of African apes, humans, and a small sample of terrestrial papionins, in which substantial abbreviation appears to have occurred. If *Proconsul* is assumed to be similar to other above branch quadrupedal anthropoids as shown here, then reduction of pedal phalangeal length, as a means of increasing hallucal opposition, is likely to have characterized the last common ancestor of *Gorilla* and humans (GLCA). Pedal phalangeal proportions are most likely to have been like those of *Gorilla* and *ARA-VP-6/500*. Human pedal phalanges are dramatically differentially reduced primarily by abbreviation of the intermediates. For further discussion, see text.

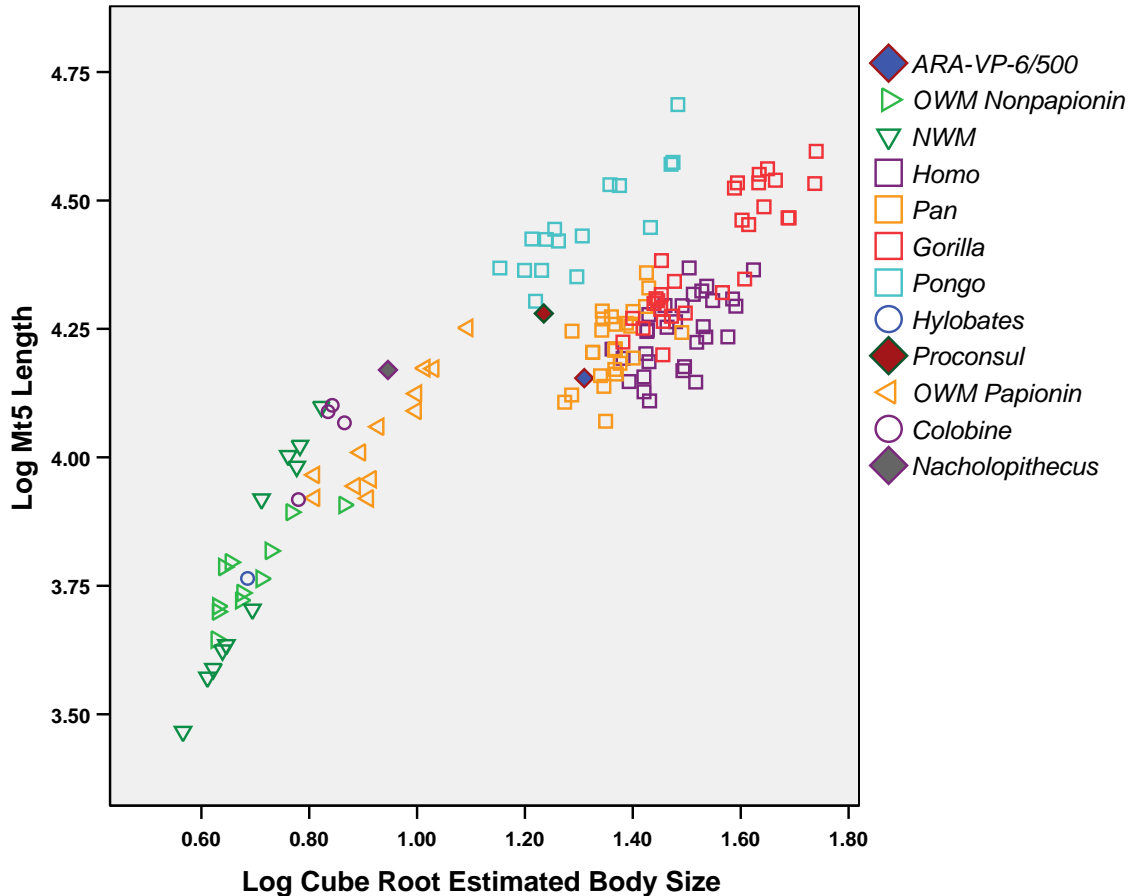


Figure S13. Posterior Metatarsal Length Relative to Body Size in Anthropoids. Natural log-log scatterplot of the cube root of estimated body mass and Mt5 length (representing the posterior metatarsus) in anthropoids. *Pan* and *Gorilla* plot in a manner suggestive of relative metatarsal abbreviation similar to that evidenced by *ARA-VP-6/500*. This strongly supports the hypothesis presented in the legend of Fig. S8, *viz.*, the metapodials of both fore- and hindlimbs were abbreviated for enhanced palmar and plantar grasping in the last common ancestor of *Gorilla* and humans (GLCA) subsequent to *Proconsul*, and that the metacarpus was then subsequently elongated for suspension independently in both African apes. This conclusion is potentially complicated by the likelihood that the Old World monkey metatarsus is not primitive, but has undergone elongation for leaping. Moreover, a point is plotted here for *Proconsul* (20), based on *KNM-RU 5872*, a substantially larger specimen than *KNM-RU 2036*, which further supports this hypothesis. Its Mt5 lacks only its head and its length was estimated as 73 mm, which must be a very close approximation. With respect to body size, the authors noted that the specimen "[i]n size conforms well with that of several female *Pan troglodytes* specimens...and was much larger than the largest male *Papio cynocephalus* we could find. A body weight of as much as 40 kg is not, then, out of the question for this individual" [(20), pp. 348-349). Only a body mass close to that of female gorillas for this specimen would contradict the hypothesis in Fig. S8. Note also that its Mt5 length/body size ratio falls within the lower boundary of *Pongo*, raising the possibility that the long digits in the latter evolved directly from a *Proconsul*-like ancestor, rather than passing through an GLCA-like stage of digital proportions.

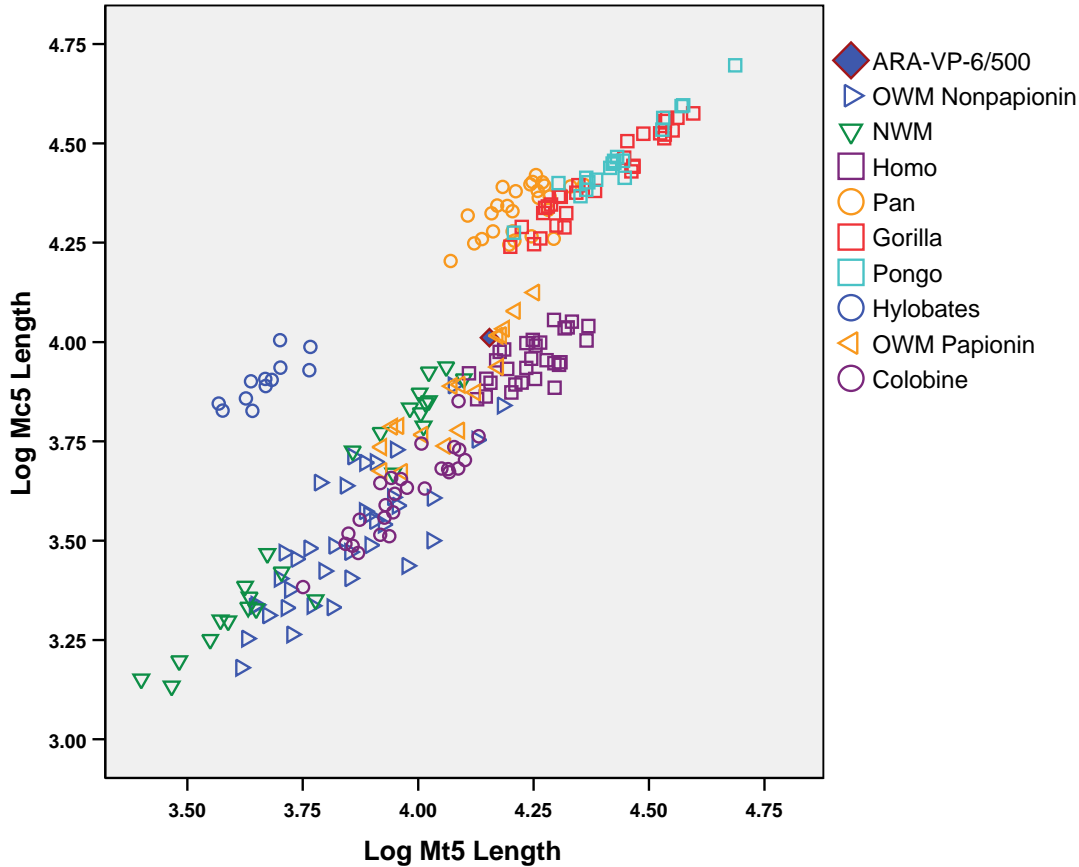


Figure S14. Metapodial Proportions in Anthropoids. Natural log-log scatterplot of Mt5 length and Mc5 length in Anthropoids. Both *Pan* and *Gorilla* Mc5s are clearly inconsistent with the hindlimb/forelimb metapodial size scaling of Old World monkeys, most of which show slight to strong metatarsal elongation (*cf.*, Fig. S13), presumably to enhance leaping capacity. These data strongly support the hypothesis presented in the legends of Figs. S8 and S13. Note the relatively primitive position of *ARA-VP-6/500*. The position of modern humans almost certainly reflects recent metacarpal reduction combined with little proportional change in metatarsal length since the proportional relationships between these two dimensions in *ARA-VP-6/500* and by extension, the last common ancestor of *Gorilla* and humans (GLCA) are very likely primitive.

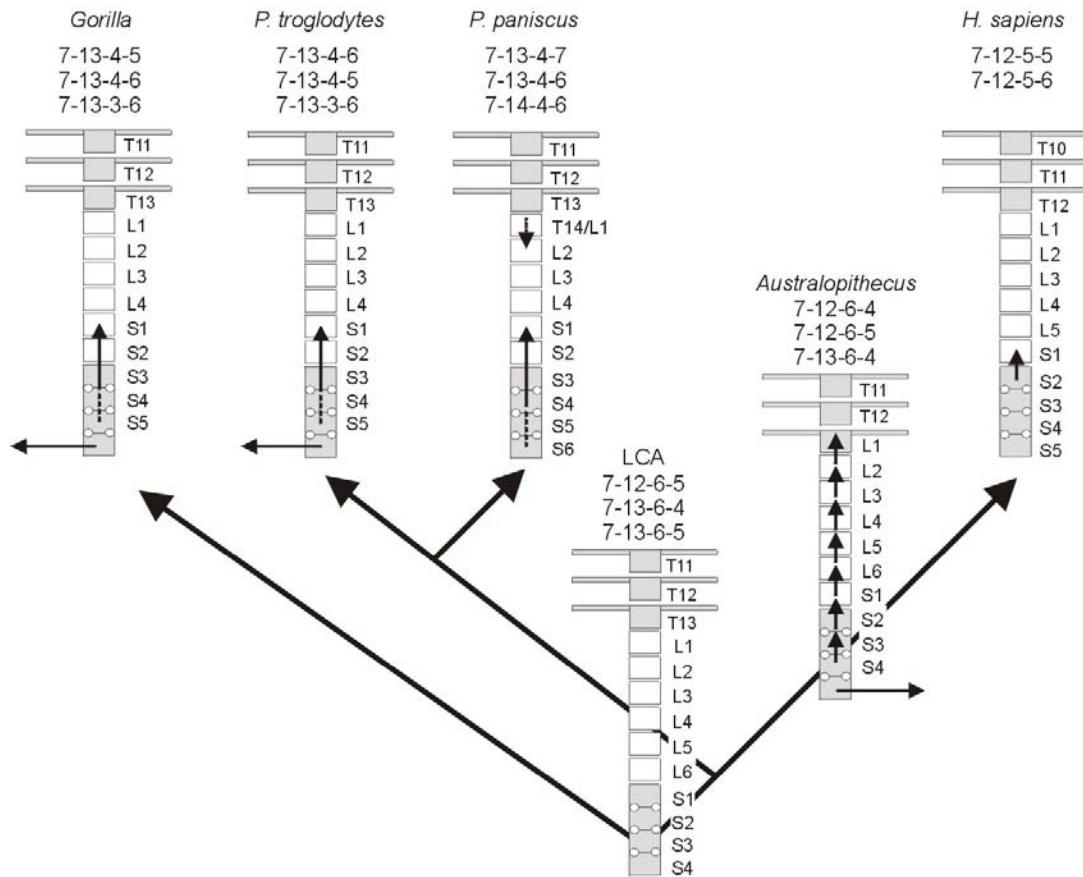


Figure S15. Reconstructed Vertebral Patterning of Hominoids (from 21). Most frequently observed axial formulas for each extant species are indicated along with the presumed modal formulas (those of highest probable frequencies) for the last common ancestor of *Gorilla* and humans (GLCA) and early hominids. A horizontal arrow indicates loss of a somite; a vertical arrow signifies changes in the positions of the anterior boundaries of *Hox* gene expression domains underlying indicated transformations of vertebral identities (22). Reduction in the number of somites contributing to the thoracic column is presumed to have occurred before the *Homo* horizon.

Table S1
Estimated Body Weight (kg) for *ARA-VP-6/500* and *A.L. 288-1*

Regression Equation Used:	<i>ARA-VP-6/500</i>	<i>A.L. 288-1</i>
All anthropoids	50.5	26.9
Female anthropoids	49.7	26.4
All hominoids (no gibbons)	52.1	22.9
Female hominoids	51.0	24.3

Table S2
Radius/Tibia of Individual Anthropoid Species

Species	Mean	N	SD
<i>Homo sapiens</i>	.65	14	.02
<i>Pan troglodytes</i>	1.11	14	.04
<i>Gorilla gorilla</i>	1.13	15	.02
<i>Pongo pygmaeus</i>	1.47	19	.03
<i>Ardipithecus ramidus</i>	.95	1	
<i>Australopithecus afarensis</i>	.93	1	
<i>Hylobates lar</i>	1.45	13	.03
<i>Proconsul heseloni</i>	.88	1	
<i>Papio papio</i>	1.04	3	.01
<i>Papio anubis</i>	1.06	7	.03
<i>Papio cymocephalus</i>	1.06	2	.01
<i>Papio hymadryas</i>	1.06	2	.03
<i>Theropithecus gelada</i>	1.01	4	.03
<i>Mandrillus sphinx</i>	.98	1	
<i>Macaca nemistrina</i>	.94	2	.04
<i>Macaca fascicularis</i>	.93	4	.01
<i>Macaca mulata</i>	.90	6	.01
<i>Macaca fuscata</i>	.92	1	
<i>Erythrocebus patas</i>	.94	5	.04
<i>Cercopithecus aethiops</i>	.84	3	.02
<i>Cercopithecus mitis</i>	.79	1	
<i>Cercocebus torquatus</i>	.86	1	
<i>Rhinopithecus roxellanae</i>	1.02	3	.004
<i>Pygathrix nemaeus</i>	1.04	2	.01
<i>Trachypithecus obscura</i>	.86	1	
<i>Presbytis rubicunda</i>	.82	1	
<i>Presbytis cristatus</i>	.84	6	.02
<i>Presbytis frontata</i>	.81	2	.05
<i>Colobus guereza</i>	.80	11	.01
<i>Alouatta belzebuth</i>	1.00	2	.03
<i>Alouatta palliata</i>	1.03	7	.02
<i>Alouatta seniculus</i>	.96	4	.03
<i>Ateles paniscus</i>	1.12	1	
<i>Ateles geoffroyi</i>	1.06	1	
<i>Ateles fusciceps</i>	1.07	5	.03
<i>Semnopithecus entellus</i>	.86	4	.04

Table S3
Hindlimb, forelimb, Mc4, and manual phalangeal lengths and indexes normalized by body mass vicar
in fossil and extant anthropoids, and by body mass in extant anthropoids

Taxon	Intermem. Index	Forelimb/ Normalizer§	Hindlimb/ Normalizer§	Phalanx / Normalizer§	Mc4/ Normalizer§	Forelimb/ Mass ^(.33) §	Hindlimb/ Mass ^(.33) §	Phalanx / Mass ^(.33) §	Mc4/ Mass ^(.33) §
<i>Ar. ramidus</i>	89-91†	31.2	34.6	2.4	3.5	143.1‡	154.7– 157.7‡	10.9‡	16.1‡
<i>Au. afarensis</i>	87-89†	34.7	38-40†			147.0‡	165.6– 168.0‡		
<i>Proconsul</i>	86.9¶								
OWM	88	36.4 (2.8)	40.1 (2.7)	2.4 (.33)	4.4 (.32)	151.1 (15.6)	173.0 (17.6)	10.5 (1.6)	18.3 (2.4)
NWM	100	43.2 (4.5)	42.8 (3.7)	3.5 (.23)	5.0 (.88)	173.2 (30.6)	178.9 (28.2)	14.5 (2.3)	20.0 (4.8)
<i>Homo</i>	69*	27.8 (1.4)	39.6 (2.0)	1.7 (.08)	2.9 (.20)	134.9	193.7	8.4	13.9
<i>Pan</i>	106*	34.3 (1.8)	32.6 (1.9)	2.7 (.17)	4.8 (.27)	159.9	147.3	12.3	22.2
<i>Gorilla</i>	114*	34.0 (2.2)	29.3 (1.6)	2.2 (.12)	4.1 (.24)	152.1	132.7	9.6	18.2
<i>Pongo</i>	138	42.5 (3.0)	30.1 (2.1)	3.5 (.24)	5.8 (.34)	191.9	139.5	15.9	26.3
<i>Hylobates</i>	130	62.0	47.9	4.6	7.2	278.1	218.2	19.7	31.1

*Hominoid taxa differ from one another by t-test at $P < .0001$

†The *ARA-VP-6/500* femur and *A.L. 288-1* tibia are not sufficiently complete for a secure length estimate. However, the crural index is stable in hominoids because almost all long bone growth occurs at both knee physes, which share the same primary *Hox* domains. These ranges are based on the highest index (*Pan*, 84), and lowest (*Homo*, 81). The *Gorilla* index is 83.

‡Based on an estimated body mass of 51.0 kg for *ARA-VP-6/500* and 28.7 kg for *A.L. 288-1*.

§Correlations between limb and bone lengths normalized by wrist-talus geometric mean (columns 2–5) and by cube roots of body mass (columns 6–9) for these seven taxonomic categories (*Ar. ramidus* not included) are 0.978 for the forelimb, 0.957 for the hindlimb, 0.980 for the Mc4, and 0.992 for the phalanges. OWM species are *M. fascicularis*, *M. fuscata*, *T. gelada*, *C. guereza*, *M. mulatta*, *M. nigra*, *E. patas*, and *P. cynocephalus*; NWM species are *A. fusciceps*, *A. paniscus*, and *A. palliata*.

|| Simple mean of the lengths of the proximal phalanges of rays 2-4 and the intermediate phalanges of rays 3-5 (chosen because each was preserved in *ARA-VP-6/500*); antimeres averaged where present.

¶From Walker and Pickford (20).

References

1. P. L. Reno *et al.*, *J Exp. Zoo. B Mol. Dev. Evol.* **310**, 240 (2008).
2. R. Ray, M. Capecchi, *Evol. Dev.* **10**, 657 (2008).
3. C. V. Ward, *Am J. Phys. Anthropol.* **92**, 291 (1993).
4. C. V. Ward, A. Walker, M. F. Teaford, I. Odhiambo, *Am. J. Phys. Anthropol.* **90**, 77 (1993).
5. C. O. Lovejoy *et al.*, *Science* **326**, 71 (2009).
6. H. Ishida, Y. Kunimatsu, T. Takano, Y. Nakano, M. Nakatsukasa, *J Hum Evol.* **46**, 69 (2004).
7. M. Nakatsukasa *et al.*, *J Hum Evol.* **45**, 179 (2003).
8. S. Almecija, D. M. Alba, S. Moya-Sola, M. Kohler, *Proc. Biol. Sci.* **274**, 2375 (2007).
9. C. O. Lovejoy, *Gait and Posture* **21**, 113 (2005).
10. R. J. Smith, W. J. Jungers, *J. Hum. Evol.* **32**, 523 (1997).
11. A. M. W. Porter, *Int. J. Osteoarchaeol.* **5**, 203 (1995).
12. B. Asfaw *et al.*, *Science* **284**, 629 (1999).
13. B. Demes *et al.*, *J. Hum. Evol.* **26**, 353 (1994).
14. K. L. Rafferty, A. Walker, C. B. Ruff, M. D. Rose, P. J. Andrews, *Am. J. Phys. Anthropol.* **97**, 391 (1995).
15. C. B. Ruff, A. C. Walker, M. F. Teaford, *J. Hum. Evol.* **18**, 515 (1989).
16. S. Ward, B. Brown, A. Hill, J. Kelley, W. Downs, *Science* **285**, 1382 (1999).
17. W. L. Jungers, *Nature* **297**, 676 (1982).
18. M. Nakatsukasa *et al.*, *J Hum Evol* **46**, 777 (2004).
19. S. Moya Sola, M. Kohler, *Nature* **379**, 156 (1996).
20. A. C. Walker, Pickford M, in *New Interpretations of Ape and Human Ancestry*, R. L. Ciochon, R. S. Corruccini, Eds. (Plenum, New York, 1983), pp. 325-413.
21. M. A. McCollum, B. A. Rosenman, G. Suwa, R. S. Meindl, C. O. Lovejoy, *J. Exp. Zool. B (Mol. Dev.)* DOI: 10.1002/jez.b21316 (2009).
22. G. P. Wagner, A. O. Vargas, *Genome Biol.* **9**, 213 (2008).